Article

'The Best of Two Worlds'—Combining Classifier Fusion and Ecological Models to Map and Explain Landscape Invasion by an Alien Shrub

Nuno Mouta [1,*] , Renato Silva [1] , Silvana Pais [1,2], Joaquim M. Alonso [1,2], João F. Gonçalves [1,2,3] , João Honrado [2,3] and Joana R. Vicente [2,3]

1   Prometheus—Research Unit in Materials, Energy and Environment for Sustainability, Instituto Politécnico de Viana do Castelo, 4900-347 Viana do Castelo, Portugal; renato.silva@esa.ipvc.pt (R.S.); silvana.pais@esa.ipvc.pt (S.P.); malonso@esa.ipvc.pt (J.M.A.); joao.goncalves@cibio.up.pt (J.F.G.)
2   CIBIO/InBIO—Research Centre in Biodiversity and Genetic Resources, Campus de Vairão, Universidade do Porto, Rua Padre Armando Quintas, 7, 4485-661 Vairão, Portugal; jhonrado@fc.up.pt (J.H.); jsvicente@fc.up.pt (J.R.V.)
3   Departamento de Biologia, Faculdade de Ciências, Rua Campo Alegre s/n, Universidade do Porto, 4169-007 Porto, Portugal
*   Correspondence: nuno.mouta@esa.ipvc.pt

Abstract: The spread of invasive alien species promotes ecosystem structure and functioning changes, with detrimental effects on native biodiversity and ecosystem services, raising challenges for local management authorities. Predictions of invasion dynamics derived from modeling tools are often spatially coarse and therefore unsuitable for guiding local management. Accurate information on the occurrence of invasive plants and on the main factors that promote their spread is critical to define successful control strategies. For addressing this challenge, we developed a dual framework combining satellite image classification with predictive ecological modeling. By combining data from georeferenced invaded areas with multispectral imagery with 10-meter resolution from Sentinel-2 satellites, a map of areas invaded by the woody invasive *Acacia longifolia* in a municipality of northern Portugal was devised. Classifier fusion techniques were implemented through which eight statistical and machine-learning algorithms were ensembled to produce accurate maps of invaded areas. Through a Random Forest (RF) model, these maps were then used to explore the factors driving the landscape-level abundance of *A. longifolia*. RF models were based on explanatory variables describing hypothesized environmental drivers, including climate, topography/geomorphology, soil properties, fire disturbance, landscape composition, linear structures, and landscape spatial configuration. Satellite-based maps synoptically described the spatial patterns of invaded areas, with classifications attaining high accuracy values (True Skill Statistic, TSS: 0.895, Area Under the Receiver Operating Curve, ROC: 0.988, Kappa: 0.857). The predictive RF models highlighted the primary role of climate, followed by landscape composition and configuration, as the most important drivers explaining the species abundance at the landscape level. Our innovative dual framework—combining image classification and predictive ecological modeling—can guide decision-making processes regarding effective management of invasions by prioritizing the invaded areas and tackling the primary environmental and anthropogenic drivers of the species' abundance and spread.

Keywords: invasive alien species; plant invasion; *Acacia longifolia*; *biomod2*; Sentinel-2; classifier fusion; supervised classification; predictive modeling

1. Introduction

Biological invasions represent a major threat to biodiversity worldwide, with a broad range of impacts on ecosystem services, natural capital, and human well-being [1]. The introduction of alien organisms in new ecosystems has grown exponentially during the last decades due to the increase of trade (on a global scale) and unprecedented mobility

of people and goods [2,3]. Driven by this reality, new and often more aggressive invasive species are expected to spread, threatening the use of natural resources.

Due to their potential impacts and associated costs, biological invasions are at the core of major global political initiatives, from the 1992 Convention on Biological Diversity (CBD) to the 2030 Agenda for Sustainable Development of the United Nations. Specific to invasions, the Aichi Target 9 from the CBD's Strategic Plan for Biodiversity 2011–2020 stipulated that "by 2020, invasive alien species and pathways are identified and prioritized, priority species are controlled or eradicated, and measures are in place to manage pathways to prevent their introduction and establishment". Successfully pursuing that goal over this new decade will require a stronger focus on mapping, predicting, and identifying potential risks and promoting action upon invaders before they become established [4].

Besides direct human management, the success of biological invasions is determined by three broad factors: the number of propagules entering the new environment, the new species' life strategy and functional characteristics, and the environment's susceptibility to invasion [5]. The invasion process is deeply influenced by the traits of receiving landscapes that promote their susceptibility to invasion by species from other world regions. Moreover, the spatial and ecological patterns of invasive plants are strongly driven by disturbance regimes acting upon ecosystems and landscapes [6].

Even though the need to enhance ecosystem services often drives plant species introductions in non-native ranges (e.g., soil fixation, erosion control, landscape aesthetics), several negative ecological, economic, and social impacts can occur if the species become invasive. In particular, woody invasive alien species can alter ecosystem processes and functions (e.g., biodiversity erosion, increased fire-proneness, allergic reactions to pollen, dense vegetation in roads or tracks, ecosystem functioning disruptions) [7–9].

Acacia species are known worldwide for their invasive characteristics [10]. In the northwest of Portugal (where the study area is located), environmental factors such as the regions' rugged topography, the high levels of precipitation and sun hours, associated with anthropological factors like rural abandonment and fire regime changes during the last decades promoted the spread of several invasive plant species of the genus Acacia, including *Acacia longifolia* (Andrews) Willd [11–13] (hereafter *A. longifolia*).

Accurate high-resolution mapping of invasive alien species is critical to pursue political initiatives, especially for anticipating, early detection, and support management options on plant invasions [14,15], and remote sensing imagery and techniques are paramount for this purpose. Multispectral sensors onboard satellite platforms, such as Sentinel-2, improve the possibilities of detecting alien plant species not only because of suitable spatial, temporal, and spectral resolutions of the sensor array but also due to the large image swath covering vast regions at once. Another advantage of Sentinel-2 is that data is available free of charge in contrast to commercial very-high-resolution platforms such as Rapid-Eye, WorldView-1-4, GeoEye-1, in which image acquisition costs are often impeditive for long-term monitoring. Sentinel-2 offers ten spectral bands covering the visible, near, and shortwave infrared at a spatial resolution of 10 to 20 m (plus three additional bands with 60 m resolution) and five days of temporal resolution. Such characteristics make Sentinel-2 suitable for invasive species mapping and assessment and allow continuous monitoring at several spatial and temporal scales [14]. These advances make possible a better detection and perception of the spectral and physical differences between alien plant species and autochthonous species/vegetation [15].

Complementarily to advances in remote sensing, new statistical and machine-learning algorithms allow to better exploit and profit from these data. The software package *biomod2* [16] is a well-established platform implemented in R that allows users to assess and combine different modeling/classification techniques based on statistical and machine-learning algorithms [17]. Designated as an ensemble platform for species distribution modeling (SDM), *biomod2* allows predicting the habitat suitability of a species across a geographic space by establishing relationships between species and environmental variables, based on statistical and machine-learning algorithms [18,19]. Despite the unquestionable

value and usefulness of SDMs, they often fall short to actually depict invaded areas and characterize several dimensions usually required by policymakers who need to quickly and accurately detect invaded places to plan interventions [20]. This happens because SDMs are correlative models, calculated from species presence/absence (or pseudo-absence) point records which are then related to environmental variables (e.g., climate, geomorphology, soil, land use) to generate a final potential distribution of a target species, often with a coarse resolution inadequate for control or management efforts [21].

However, the *biomod2* R package can also be applied to perform pixel-based supervised classification through an ensemble approach, which in the context of remote sensing image analysis and data mining science, is known as "classifier fusion" or "stacking" methods [22]. These techniques allow the combination of different supervised classification algorithms to obtain a final consensus capable of discriminating the presence/absence of a species based on satellite spectral data. As such, *biomod2* can be used as a suitable multi-classifier stacking ensemble, which allows standardizing the uncertainty present in the individual models and determines a general prediction consistent with all classification methods [16,23]. Another advantage of combining spectral data in *biomod2* for alien plant species mapping relates to its ability to run non-parametric models that, unlike parametric models, can assume that a pixel is a mixture of features and sub-divide each one to increase spectral variance inside and between pixels [24].

In addition to fast-paced advances in remote sensing satellite platforms and accessibility of its data, predictive models in ecology, and especially in invasion biology (e.g., [9,25]) are also growing and diversifying their applications. Predictive modeling is the process of applying a statistical model or machine-learning algorithm to data to predict an outcome or to capture the association between the outcome (e.g., presence/absence or abundance of a species) and a set of drivers as defined by [26]. This analytical toolkit, supported mainly by statistical and machine-learning algorithms, allows for inferences regarding multi-scale invasion drivers (either invasibility or invasiveness) and obtain spatiotemporal predictions [8]. Overall, these advances manifest in managers' and stakeholders' ability to profit from the availability of data and analytical routines to make better assessments, monitor, and devise strategies to control invasive species. Despite these advances, the combination of both satellite image classification (for invasive species mapping/detection) and predictive modeling (for inferring invasion drivers) has been seldom explored (but see, e.g., [27]). As such, researchers miss the ability to profit from synergistic advances of both fields and obtain more insights regarding species invasions.

Aiming to address this gap, in this study we developed and tested a dual methodological framework for assessing landscape invasion by alien woody plants. The framework is illustrated for landscape invasion by the Golden wattle (*Acacia longifolia*) in a municipality of Northern Portugal. First, we developed an improved mapping approach based on Sentinel-2 imagery and stack fusion techniques with the R package *biomod2* to generate a spatially explicit representation of invaded areas. Secondly, we used a predictive model-based procedure with the Random Forests algorithm to assess the influence on the invasion process of several hypothesized drivers related to (i) (bio-)climate, (ii) topography/geomorphology, (iii) soil properties, (iv) fire disturbance, (v) land use/landscape composition, (vi) linear landscape elements, and (vii) landscape pattern/configuration. We discuss the relevance of the proposed approach—combining satellite image classification and predictive ecological modeling—to manage invasive alien species at an appropriate scale to guide decision-making processes.

2. Materials and Methods

2.1. General Workflow

To address the challenges of mapping the invasive alien plant species *A. longifolia* and identify the key drivers underlying the spread and abundance at the landscape level, we propose and develop a dual approach. In stage one (see Section 2.5, Section 2.6, Section 2.7, Section 2.8), supervised image classification (supported by classifier fusion) was used to

map the extent of invasion by the target species based on Sentinel-2 data. In stage two (see Section 2.9), predictive modeling was used to underpin and rank the importance of the main drivers of the species invasion. This last component of the workflow relied on a landscape-level approach, supported by previous results from stage one (i.e., invaded areas map) and a hexagon tessellation of the whole study area. This workflow enabled us to assess which environmental factors, and respective drivers, mainly contribute to the spread of the species. Specific steps of each stage are described in Figure 1 and detailed in the subsections below.
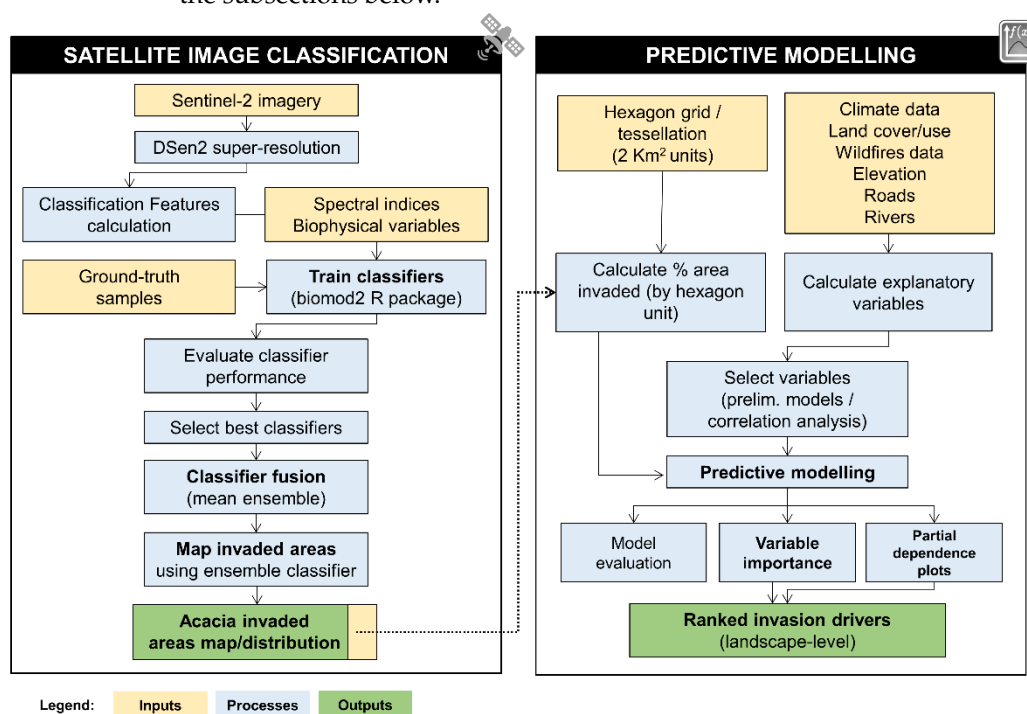

Figure 1. General workflow proposed for addressing *A. longifolia* mapping and landscape-level drivers combining satellite image classification (**left-side**) and predictive modeling (**right-side**).

2.2. Target Species

In general, Australian Acacia species are known for their phenotypic plasticity and invasive abilities, promoting a wide range of impacts, causing a general reduction in ecosystem services delivery [28]. These species spread impacts on public health (e.g., allergies) [29,30], decrease in the water availability (either by the traits of the plant or by the density) [31], modification on the biogeochemical cycles [32–34], homogenization of ecosystems composition and structure [35], change of fire regimes and competition with native species [10].

Specifically, the target species *A. longifolia* was introduced in Portugal for ornamental purposes and for fixing soils in eroded areas [36]. In particular, this species is known to spread along the coastline, degraded areas, and through the margins of low-altitude rivers. Together with the increasing human pressure in these specific areas, the resilience and natural value has severely decreased [37,38]

Due to *A. longifolia* traits, such as rapid growth, regeneration capacity (sprouting vigorously), reaction to disturbing agents (fire), remarkable ability to compete for resources, production of viable seeds for decades, absence of competitors and natural predators, this species is an aggressive invader in the study area [39].

2.3. Study Area

The study area is located in the municipality of Viana do Castelo (NW Portugal), which has an area of 319.02 km^2 and 85,445 inhabitants. The region presents a temperate climate, with an average annual temperature of 14.5 °C and an average annual rainfall of

1264 mm [40]. With a remarkable geomorphological and landscape heterogeneity marked by three distinct landscape units: mountain, riverside, and coastline, its rugged topography (from sea level to a maximum elevation above 800 m) make this region unique for its diversity and specific habitat types associated with high levels of biodiversity [40].

In the study area, *A. longifolia* is spread in large areas, some of them classified as Natura 2000, causing ecological impacts and promoting ecological regime changes (e.g., alteration of the forest composition of riparian galleries) [41]. Furthermore, the study area presents a set of socio-ecological conditions which facilitate the species expansion, such as the current regime of very frequent rural fires, large seed banks, and a very dense corridor network (associated with communication roadways) (Figure 2).
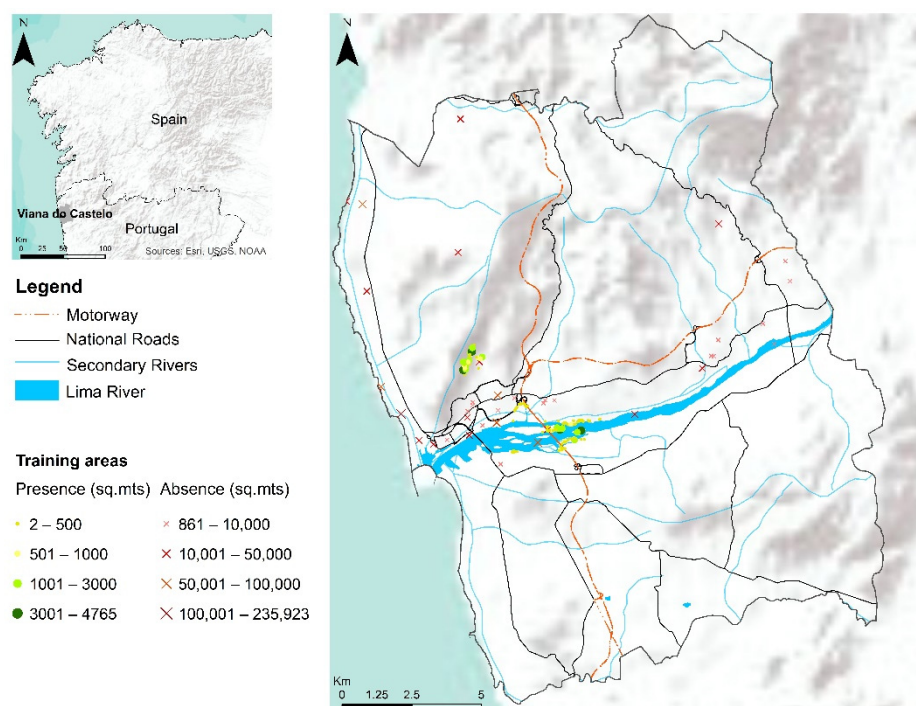

Figure 2. Location of the study area. Points represent the presence (green color) and X's absence (in red) areas used for training the supervised classifier with a size proportional to the symbol dimension.

2.4. Occurrence Data

The delimitation of training areas is of great importance for obtaining accurate results. The *biomod2* classification algorithms are characterized by having binomial responses (distribution values between 0 and 1), where 0's code absences of *A. longifolia* and 1's denotes its presence. The diversity of natural spaces and their land uses creates several challenges for identifying spatial and spectral signatures for *A. longifolia*.

To represent the environmental heterogeneity on the study area, a total of 207 training areas were considered, covering river margins, mountainous areas, seaside, and urbanized spaces, always having the attention to record especially significant training areas (i.e., combining mixed pixels but most often heavily invaded areas which generate 'pure' pixels for training). Several sites representing the study area's main land cover types (e.g., urban, forest, motorway, shrublands, and agricultural areas) were inspected to collect training samples. Through ground surveys and GPS equipment, sites invaded with considerable dimensions (>5 m^2) were recorded and georeferenced ($n = 67$). Due to some locations' inaccessibility, GIS tools and orthophoto maps with high-spatial-resolution (0.3 m) were used to obtain additional presence areas ($n = 100$). Additionally, through manual photointerpretation of high-resolution images, several areas representing the main land cover types for the study area were collected and used as absences (i.e., 'true-absences'; $n = 40$). The

overall median size of training areas is 188 m^2, while the median size of presence areas is 112 m^2 and 13,820 m^2 for absence areas.

To better represent the spectral variance in the image stack and complement the data from true-absences, three sets of pseudo-absences were randomly generated throughout the study area using *biomod2*'s internal routines. To balance train data and avoid biasing the accuracy of model predictions [42], the number of pseudo-absences was set equal to the number of presences.

2.5. Satellite Remote Sensing Data

Sentinel-2A multispectral data, provided by the Copernicus Open Access Hub, was analyzed and inputted in the classification workflow. We collected one image per month between December 2018 to May 2019, covering the final stage of the growing season (December–January), flowering period (January–March), and post-flowering period (April–May). To increase accuracy, it is necessary to minimize overall cloud cover in collected images from the study area. For each of the six days analyzed, we collected imagery with 13 spectral bands (Top-Of-Atmosphere Level L1C) that were transformed into the atmospherically corrected L2A product through the sen2cor processing software for better comparability, spectral quality, and increased signal retrieval [43], thus creating 12 available bands.

Through the DSen2 super-resolution algorithm [44], the spectral bands at 20 and 60 m were resampled to 10 m through a pre-trained deep neural network implementing this method, attaining better performance than standard resampling methods [44]. The improved and rescaled bands were then used to calculate, for each month, several spectral vegetation indices: Normalized Difference Vegetation Index (NDVI), Enhanced Vegetation Index (EVI), Modified Chlorophyll Absorption in Reflectance Index (MCARI), MERIS Terrestrial Chlorophyll Index (MTCI), and the second Modified Soil Adjusted Vegetation Index (MSAVI2). For higher accuracy on the vegetation index calculation, specific formulas for Sentinel-2A bands were employed [45] (Table 1).

Table 1. List of spectral vegetation indices and biophysical variables used to support *A. longifolia* supervised classification and mapping.

Index	Explanation	Specific Formula
NDVI	Enhances vegetation differences photosynthetically [46]	$\frac{(b8 - b4)}{(b8 + b4)}$
EVI	Distinguish differences in the canopy structure, architecture, and physiognomy [47,48]	$2.5\frac{b9 - b5}{(b9 + 6b5 - 7.5b1) + 1}$
MCARI	A measure of the leaf chlorophyll content enhancing vegetation differences [49]	$((b5 - b4) - 0.2(b5 - b3))\left(\frac{b5}{b4}\right)$
MTCI	Enhances vegetation senescence and water/nutritional stress [50]	$\frac{(b6 - b5)}{(b5 + b4)}$
MSAVI 2	Retrieves information about vegetation dynamics and reduced the soil background variations [51]	$\frac{2b9 + 1 - \sqrt{(2b9 + 1)2 - 8(b9 - b5)}}{2}$
LAI	Measure for the total area of leaves per unit ground area [52]	S2 SNAP Toolbox biophysical processor.

The Leaf Area Index (LAI) was calculated through the software SNAP with the original 12 bands. In total, 18 spectral layers (12 bands and 6 indexes) were considered for each month (totaling *n* = 108).

2.6. Biomod2 Multi-Algorithm Supervised Classification Training and Evaluation

The study was performed using the latest version of the *biomod2* package (version 3.4.6) within the statistical software R (R Development Core Team 2012) version 4.0. This analysis is supported by several supervised classification algorithms, based either on statistical or machine learning methods, including Generalized Linear Model (GLM), Flexible Discriminant Analysis (FDA), Gradient Boosting Machine (GBM), Random Forest (RF); Classification Tree Analysis (CTA), Generalized Linear Model (GAM), Artificial Neural Network (ANN), and MAXENT, Phillips (MAX).

For the input dataset, three different sets of pseudo-absences and 30 model repetitions were performed using the default options of *biomod2*. For evaluating the performance of the classifiers, holdout cross-validation was used by setting 80% of the dataset for training and 20% for evaluation purposes. Additionally, we ensured a prevalence of 0.5, which means that the presences and the pseudo-absences have the same weight in the model calibration process.

To evaluate the overall performance of either partial and final ensemble/fusion classifiers for the test fraction (i.e., not used for training), we calculated the True-Skill Statistic (TSS), Cohen's Kappa (KAPPA), and the area under the Receiver Operating Curve (ROC). The first two measures vary from [−1, 1] while the second between [0, 1]. Values closer to one flag better-performing classifiers and higher discrimination ability. To complement these measures, we also calculated sensitivity and specificity. Sensitivity is the proportion of observed presences predicted and, therefore, quantifies omission errors, while specificity is the proportion of observed absences that are correctly predicted and therefore quantifies commission errors. Overall, sensitivity is the probability that the classification algorithm will correctly classify presences, whereas specificity is the probability that the model will correctly classify absences.

2.7. Variable Reduction and Importance Calculation

Considering that *biomod2* demands considerable computational resources, especially when the number of variables (or features) used is high, a preliminary reduction was performed. To identify critical variables in the model's preparation and thus reduce the total number of variables, we analyzed the importance of each through a set of preliminary modeling steps using six classification techniques: GLM, FDA, GBM, RF, CTA, and MAX. Variable importance calculation was performed using *biomod2*'s function variables importance, which returns each variable's importance score. The highest the value, the more influence the variable has on the supervised classification process. A value of 0 assumes no influence of a variable, whereas values closer to 1 signal a highly important variable [17]. This variable importance analysis allowed selecting the variables with higher importance, making the classifier fusion less computationally demanding [53]. We considered the best 17 individual variables to maintain a good ratio between performance and complexity (Appendix A).

2.8. Classifier Fusion Ensemble

An ensemble fusion model was obtained by calculating the weighted mean (by the TSS performance score) of selected partial classifiers, i.e., those which got a good to excellent performance considering a rule of TSS > 0.8. Finally, to convert the ensemble classifier model result from probability/suitability values (i.e., continuous values within the [0, 1] range) to a binary outcome (species presence: 1 or absence: 0), we applied a numerical threshold [54,55]. In our case, we defined this "binarization" threshold as the value which maximizes the TSS score [56].

Values lower than the TSS cutoff were considered pixels with very low spectral similarity to invaded areas, whereas *biomod2*'s output values close to the maximum rescaled probabilistic value of 1000 were considered to have very-high spectral similarity to invaded areas.

2.9. Assessing the Invasion Drivers of A. longifolia at the Landscape Level through Predictive Modelling

From the classified Sentinel-2A images, we assessed the abundance drivers of *A. longifolia* through a predictive model-based framework based on the Random Forest regression algorithm [57]. We started by devising a hexagonal grid (or tessellation) covering the whole study area with 2 Km² units for performing this assessment. This grid was necessary to adequately address the structural and environmental drivers promoting the abundance of *A. longifolia* at the landscape level. The size of each hexagonal unit was considered suitable for three relevant criteria: (i) maximize the environmental heterogeneity, (ii) scale conformity to climate data (which is the coarser dataset with ~1 Km² of spatial resolution), and (iii) adequate sample size for modeling (*n* = 189 effective units after checking for invalid data).

The response variable is the proportion covered by invaded areas for each hexagon unit, obtained from zonal statistics of the classified Sentinel-2A imagery from previous steps. The *A. longifolia* map generated through image classification was used to quantify the response variable, allowing to get a full area view of invasion extent at the landscape level instead of relying on a limited set of sample training areas for that purpose.

The list of predictive drivers (Table 2), exploits the following aspects of distribution and colonization of *A. longifolia* at the landscape level, which relate to the degree of invasibility [8].

Table 2. Full list of environmental factors considered, which were hypothesized as drivers of invasion in the study area, totaling 59 independent variables (see also Appendix B). Variables in bold were selected for the final RF regression model (*n* = 20).

Environmental Factors	Driver Description	Acronym
(Bio)Climate	Annual Mean Temperature	CL_BIO01
	Mean Diurnal Range	CL_BIO02
	Isothermality	CL_BIO03
	Temperature Seasonality	**CL_BIO04**
	Maximum Temperature of Warmest Month	CL_BIO05
	Minimum Temperature of Coldest Month	**CL_BIO06**
	Temperature Annual Range	CL_BIO07
	Mean Temperature of Wettest Quarter	CL_BIO08
	Mean Temperature of Driest Quarter	CL_BIO09
	Mean Temperature of Warmest Quarter	CL_BIO10
	Mean Temperature of Coldest Quarter	CL_BIO11
	Annual Precipitation	CL_BIO12
	Precipitation of Wettest Month	CL_BIO13
	Precipitation of Driest Month	CL_BIO14
	Precipitation Seasonality	**CL_BIO15**
	Precipitation of Wettest Quarter	CL_BIO16
	Precipitation of Driest Quarter	CL_BIO17
	Precipitation of Warmest Quarter	**CL_BIO18**
	Precipitation of Coldest Quarter	CL_BIO19

Table 2. *Cont.*

Environmental Factors	Driver Description	Acronym
Disturbance	Total Burnt Area (last 10 years)	DT_BA10YR
	Total Burnt Area (last 20 years)	DT_BA20YR
	Total Burnt Area (last 5 years)	**DT_BA5YR**
Land use	Percent of permanent crops	LU_PCPCO
	Percent of annual crops	**LU_PCACO**
	Percent of permanent and annual crops	LU_PCPAC
	Percent of native forests	LU_PCNFO
	Percent of eucalyptus (production) forest	**LU_PCEFO**
	Percent of maritime-pine (production) forest	**LU_PCPFO**
	Percent of shrublands	**LU_PCSHL**
	Percent of complex agroforestry mosaics	LU_PCAFM
	Percent of other production forests	**LU_PCOPF**
	Percent of pasturelands	LU_PCPAS
	Percent of wetlands	LU_PCWET
	Percent of beaches and sand dunes	LU_PCBSD
	Percent of roads and rails	LU_PCRRL
	Percent of bare rock surfaces	LU_PCBRS
	Percent of water surfaces	LU_PCWTS
	Percent of artificial/urban areas	**LU_PCART**
	Percent of sparsely vegetated areas	LU_PCSPV
Landscape pattern/configuration and heterogeneity	**Landscape Mean Patch Area**	**LP_MNPAR**
	Landscape Patch Area Coefficient of variation	**LP_PACOV**
	Landscape Largest Patch Index	LP_LAPAI
	Landscape Shannon Diversity	LP_SHDVI
	Landscape Simpson Diversity	**LP_SPDVI**
	Landscape Patch Area Standard-deviation	LP_PASTD
Linear elements	Landscape edge density	LE_EDGDN
	Total length of rivers	**LE_TLRIV**
	Total length of all road types	LE_TLROD
	Total length of motorways	**LE_TLMTW**
Soil properties	**Available water content**	**SO_AVWTC**
	Bulk Density	SO_BULKD
	Percent of clay in soils	**SO_PCLAY**
	Percent of coarse elements in soils	**SO_PCOAR**
	Percent of sand in soils	SO_PSAND
	Percent of silt in soils	SO_PSILT
Topography/ Geomorphology	Slope (%)	TG_SLOPE
	Average Solar Radiation	**TG_RADAV**
	Topographic Ruggedness Index	TG_TORGI
	Topographic Wetness Index	TG_TOWTI

To select a smaller and meaningful set of predictive drivers, we performed an iterative variable elimination procedure combining variable importance obtained from an initial set of Random Forest models ($n = 500$) and multicollinearity reduction through non-parametric Spearman correlation analysis. From this analysis, we retained the 20 most important drivers with a pairwise correlation of $\rho < |0.75|$. This number of drivers was chosen to include at least one variable from each of the seven groups of drivers (see Appendix B for the complete list).

Model evaluation, for the final model including the selected set of predictive drivers, was based on the Out-Of-Bag (OOB) fraction [57,58], which consists of the subset of records not selected for training through bootstrap resampling in RF. Based on this, the following evaluation metrics were calculated: R-squared (R^2), Spearman Correlation (CORSP), Root-Mean-Square Error (RMSE) and, the Median Absolute Error (MAE).

Drivers' importance ranking was assessed through multiple runs of RF ($n = 1000$) and calculating the percentage increase in mean square error by shuffling the OOB samples' values. For each tree, the prediction error on OOB samples is calculated through the mean-square error. After that procedure, the same is performed after permuting each predictor driver. The difference between the two is then averaged over all trees and normalized by the standard deviation of the differences to obtain the final importance measure. Importance values across all rounds were averaged. To increase the random forest model interpretability, we developed partial dependence plots [59], which can be defined as low-dimensional graphical representations of the prediction function so that the relationship between the outcome and each predictor can be more easily visualized and interpreted. These plots are especially useful for explaining the output of "black-box" models such as the random forest model.

3. Results

The results obtained supported the spatially explicit detection of areas invaded by *A. longifolia*. The supervised image classification performance through *biomod2*'s revealed a good ability to map the target species.

Preliminary analysis aiming to reduce the number of variables employed in the image classification stage allowed for some performance gains while also making it less demanding in computation time. The results obtained by the variable importance analyzes can be consulted in Supplementary Information—Tables S1 and S2. In addition, the development of a predictive model based on the mapping carried out in the first stage, and the main environmental variables allowed identifying drivers of invasibility.

3.1. Partial and Ensemble Fusion Classification Performance

The supervised classification technique with the best results for all evaluation metrics was GAM, followed by the FDA and RF algorithms. In contrast, the classification technique ANN presented the lowest scores across all classifiers (Table 3). On average, across all partial classifiers, we found high-performance scores with 0.794 for TSS, 0.945 for ROC, and 0.798 for KAPPA.

Overall, the ensemble classifier based on *biomod2*'s multi-algorithm fusion showed very high-performance values as well as sensitivity and specificity (Table 4). The ensemble model presents a performance gain for any evaluation metric value compared to the best partial classification model (i.e., GAM). This gain shows the added value of fusing multiple classifiers with distinct types of algorithmic frameworks (i.e., such as tree-based in CTA or RF vs. neural networks in ANN).

Table 3. Partial evaluation scores by classification algorithm showing the average and standard deviation (across evaluation rounds). Numbers in **bold** indicate the top-three algorithms in our study.

Classification Algorithm	TSS		ROC		KAPPA	
	Average	Standard Deviation	Average	Standard Deviation	Average	Standard Deviation
GBM	0.799	0.042	0.953	0.014	0.796	0.042
RF	**0.824**	0.043	**0.962**	0.012	**0.823**	0.043
CTA	0.715	0.045	0.886	0.027	0.715	0.045
GLM	0.789	0.068	0.928	0.051	0.800	0.069
FDA	**0.827**	0.030	**0.964**	0.009	**0.831**	0.030
ANN	0.640	0.057	0.859	0.033	0.646	0.057
MAX	0.726	0.045	0.890	0.025	0.731	0.045
GAM	**0.843**	0.031	**0.965**	0.011	**0.846**	0.030

Table 4. Performance evaluation scores for the final ensemble classifier combining *biomod2* algorithms.

Evaluation Metric	Evaluation Metric Value (Test)	Cutoff Threshold	Sensitivity	Specificity
TSS	0.895	539	96.0	93.4
ROC	0.988	544	96.0	93.5
KAPPA	0.857	724	88.7	96.7

3.2. Feature Importance in Image Classification

According to *biomod2* ranking, the four most important variables were Band 3 (green), Band 12 (SWIR2), Band 2 (blue), and the LAI index. In opposition, the bands with lower importance were in the spectral region of red (band 4), red edge (bands 5, 6 and, 7), and the near infrared (bands 8 and 8a), often used for remote sensing of vegetation. Overall, the variable importance analysis highlighted the usefulness of the spectral bands on the classifier (with 78% of all information used) in contrast to the less performant vegetation and biophysical indices (with 22%) (Figure 3). Despite exhibiting lower importance scores and secondary contributions, the remaining variables also improved overall accuracy.
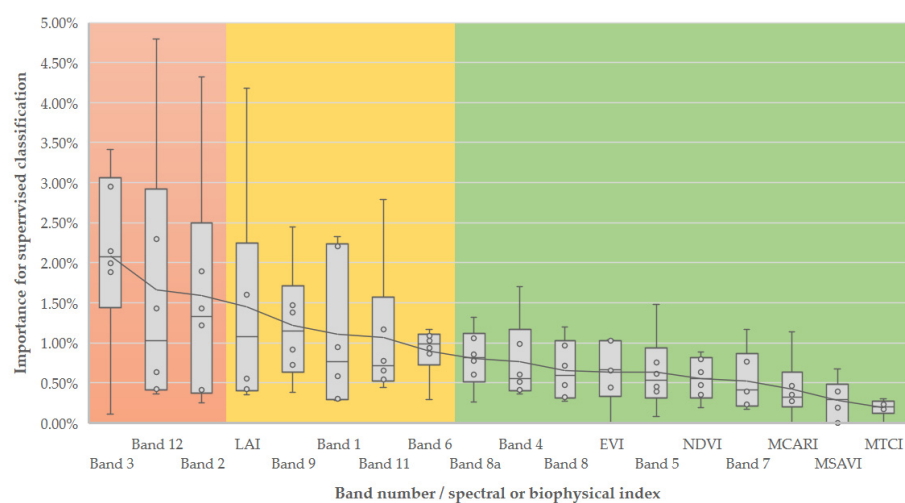

Figure 3. Boxplots showing the distribution of variable importance scores across classification algorithms and evaluation rounds sorted according to their average importance scores (each different background color represents approximately 33% of aggregated importance).

The selection of the most important variables (to reduce the computational processing time) resulted in 17 layers of spectral information with a combined relative importance of approximately 45%. The three most important independent variables were band 12 (SWIR band 2) in December (4.79%), band 2 (blue) in January (4.32%), and LAI in January with (4.18%).

The months with the highest combined relative importance (from the 17) were December, January, February (Appendix A), which coincides with the final growing period and the flowering period. On the other hand, April and May were the months with smaller contributions to the classification process (Figure 4).
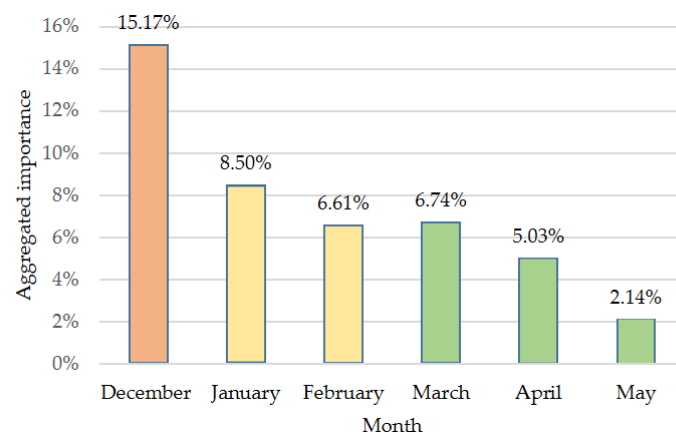

Figure 4. Relative importance by month obtained from the variable selection stage and sorted according to their aggregated scores (each color represents a similar amount of aggregated importance).

3.3. Acacia Longifolia Mapping

The ensemble classifier based on the *biomod2*'s ensemble fusion approach was able to discriminate invaded areas by *A. longifolia* spectrally similar to training sites. These areas occur along the Lima and Minho River (with higher density when approaching estuarine spaces), coastal areas, low altitude slopes with high solar exposure and smooth inclination, and discontinuous urban areas (Figure 5).

The distribution pattern *A. longifolia*, in the study area, coincides primarily with spaces of high ecological value under protection networks (e.g., Natura 2000).

3.4. Predictive Modelling—Landscape-Level Drivers of A. longifolia Invasion

After performing the preliminary models and correlation analyses, 20 predictive drivers were selected to include in the final model out of 59 (see Supplementary Information —Table S3 for all variable importance rankings). These drivers are for the climate the Temperature Seasonality (CL_BIO04), Minimum Temperature of the Coldest Month (CL_BIO06), Precipitation Seasonality (CL_BIO15), and Precipitation of the Warmest Quarter (CL_BIO18). For topography/geo-morphology, it includes Average Solar Radiation (TG_RADAV), while for soil properties, the available water content (SO_AVWTC), percentage of clay (SO_PCLAY), and percentage of coarse elements (SO_PCOAR). As for disturbance, solely the Total Burnt Area in the last five years (DT_BA5YR) was selected. Land use and landscape composition include the percentage of annual crops (LU_PCACO), percentage of eucalyptus (production) forest (LU_PCEFO), percentage of maritime-pine (production) forest (LU_PCPFO), percentage of other types of production forest (LU_PCOPF), percentage of shrublands (LU_PCSHL) and percentage of artificial/urban areas (LU_PCART) while for linear structures the Total length of rivers (LE_TLRIV) and, Total length of motorways (LE_TLMTW) and, finally, for landscape pattern/configuration the Landscape Mean Patch Area (LP_MNPAR), Simpson's Landscape Diversity (LP_SPDVI), and the Patch Area Coefficient of variation (LP_PACOV).
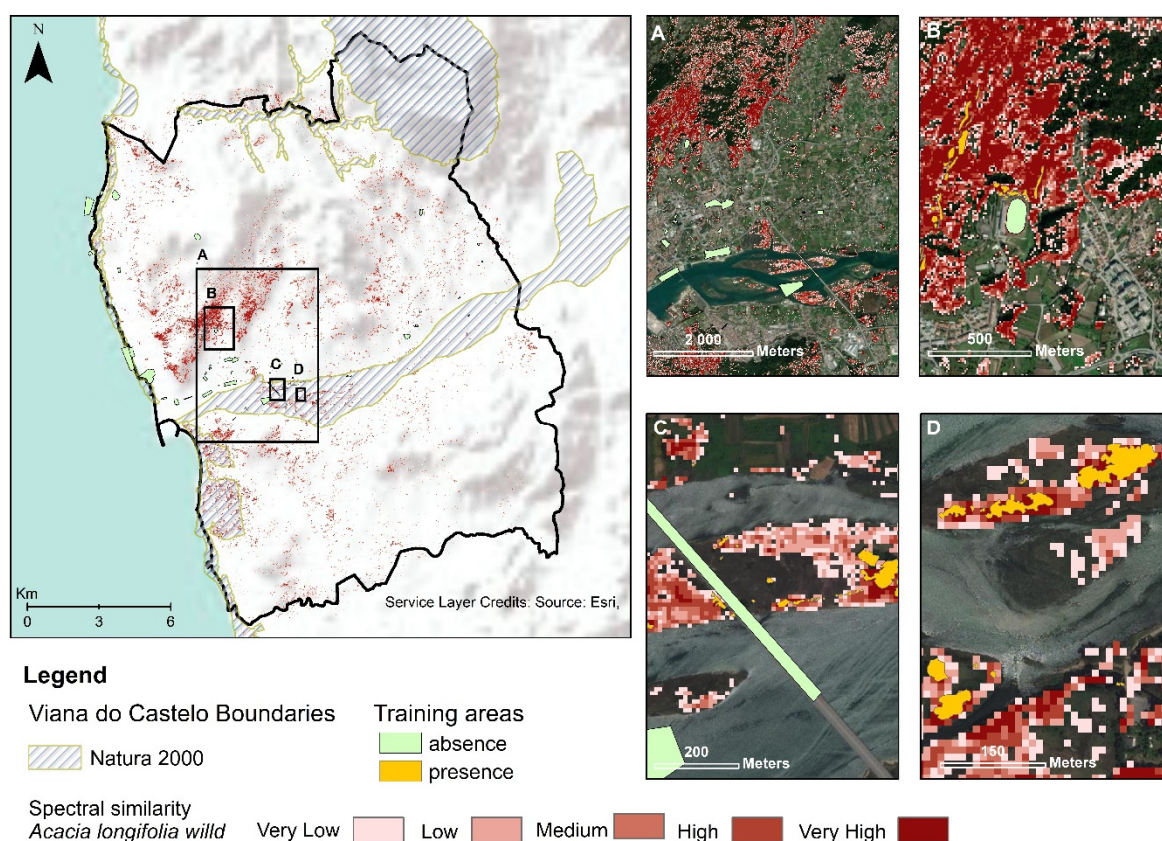
Figure 5. Map showing the distribution of invaded areas by the target species (colored pixels) obtained by the ensemble classifier. Inside these areas, the color ramp highlights the spectral similarity to invaded (train) areas, showing those spots with a potential greater likelihood of invasion or higher plant density/coverage. Training areas are shown in colored polygons in yellow color (presences) and light green (absences). Sub-areas A–D (left side) are shown in detail on the right side to depict different invaded sites from forest areas to wetlands in the stud area.

Overall, model performance for the selected drivers was generally good for the OOB test fraction with a coefficient of determination R^2 of 0.52 and a Spearman correlation between predicted and observed values of 0.76. The MAE and RMSE have an error between 3.8 and 5.5% which is considered acceptable given the response variable distribution (min: 0.0%, max: 57.5%, mean: 7.3%, standard deviation: 7.7%).

The random forest model importance (Figure 6) allowed ranking the selected drivers, which highlighted first the role of climate followed closely by land use and landscape spatial configuration (see Supplementary Information—Table S4 for driver importance ranking for the 20-best selected). We found that drivers related to soil properties, topography, disturbance, and linear elements in the landscape had comparatively less importance. Besides importance scores, partial dependence plots (Figure 7) allowed us to deepen the interpretation of each predictive driver of *A. longifolia* invasion extent at the landscape level.

More specifically, invaded areas were positively related to higher annual minimum temperature values and higher precipitation seasonality and negatively associated with temperature seasonality and the precipitation of the warmest/summer quarter (see Figure 7 and Supplementary Information—Figure S1 for all plots).

For land use/landscape composition, production forests of all types (i.e., eucalyptus, pine, and other less common types), which dominate the tree strata in invaded areas, were all positively related to invaded areas. In contrast, shrublands and annual crops were negatively related. Artificial areas showed a complex response, with invaded areas peaking at small values (i.e., probably related to forest-like landscapes) and again increasing at high values (i.e., urbanized landscape as the dominant matrix with semi-natural habitats dispersed).

As for landscape pattern/configuration, highly invaded areas tend to have larger patches (potentially dominated by continuous forest areas of a single type, e.g., monocultures of eucalyptus, maritime pine, or other dominant tree species). This effect can also be observed in the Simpson Landscape Diversity index, which is negatively related to the percentage cover of invaded areas, showing that less heterogeneous areas create favorable conditions for the target species spread.
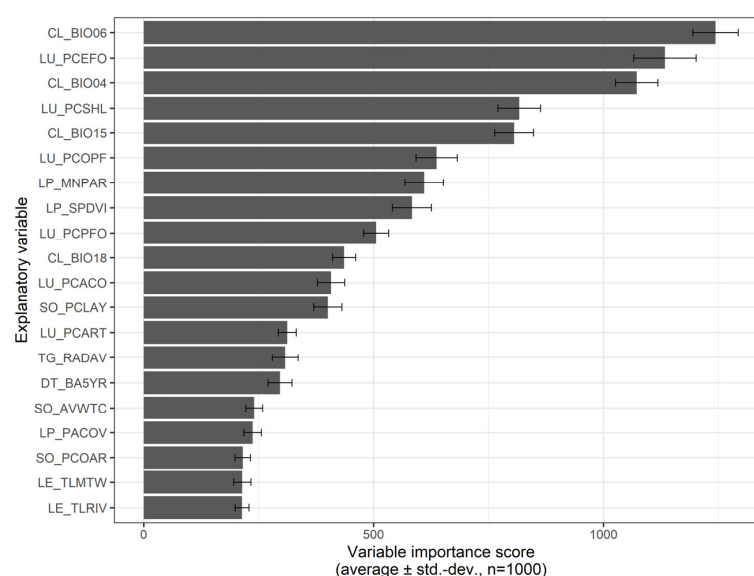

Figure 6. Importance scores for the 20-selected predictive variables calculated from the Random Forest model. Average (grey bars) and standard deviation values ('whiskers') are presented for the 1000 rounds performed with the random forests algorithm. Acronyms for predictor variables are presented in Table 2.

In terms of soil attributes, the species was positively related to soils with higher clay content and a lower percentage of coarse elements. Solar radiation (which is modulated by topography and exposure) was positively associated with the species. Disturbance dynamics related to wildfires (calculated as the total burnt area in the five past years) positively contributed to species abundance. Linear elements traversing the landscape, including both natural features (i.e., rivers) and artificial ones (i.e., motorways), also showed positive effects contributing to the landscape-level abundance of *A. longifolia*.
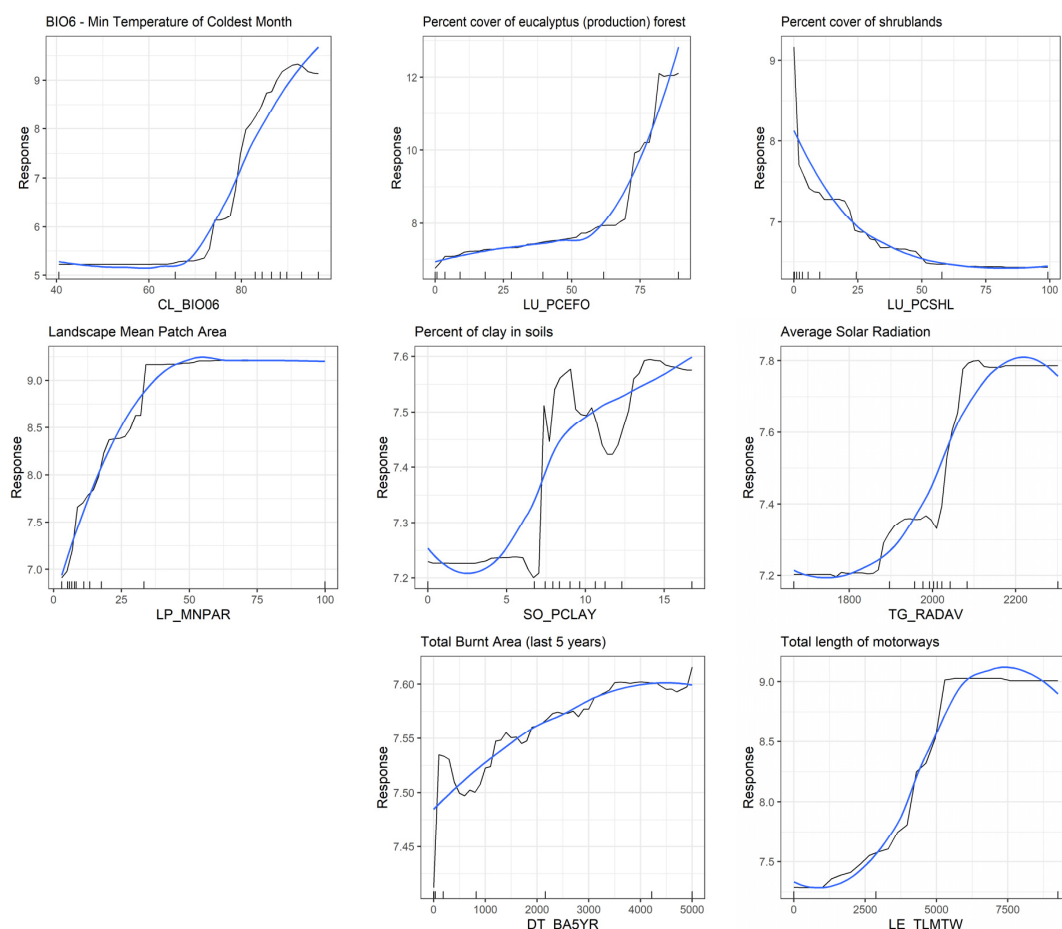
Figure 7. Partial dependence plots showing the relation between the response variable (abundance given by the percentage of invaded area in the *y*-axis) and the selected predictive variables of different environmental factors (*x*-axis). The black line indicates the "raw" response from the RF model, while the blue line applies a moving average smooth.

4. Discussion

4.1. Multispectral Remote Sensing Imagery and Data Fusion Techniques through biomod2 for A. longifolia Detection

Although distribution maps of invasive alien plants are common in scientific literature, due to the requirements and the fine-scale of species-level mapping, most resort to very-high-resolution satellites (≤5 m), airborne or unoccupied aerial vehicles to collect remote sensing data [60,61]. These data and techniques are often associated with considerable economic investments, low temporal resolutions, and time-demanding procedures (both in personal and computational terms). Spatially explicit maps of invasive alien plants are critical to understanding their spatiotemporal distribution patterns and their driving factors at several scales to support and improve management and control strategies.

For tackling this challenge, satellite remote sensing coupled with classifier fusion methodologies (such as the one employed here through the *biomod2* R package) offers tremendous advantages [62]. First, this methodology is implemented on the R computing platform, firmly established in the academic community. Second, multispectral and multitemporal high-resolution imagery is free of charge (e.g., Sentinel-2, Landsat), allowing continuous updates of invasive alien plant species' distribution maps. Moreover, contrary to species distribution models, which target invasive alien plant potential distribution, satellite image classification does not require environmental variables at low spatial resolution (e.g., precipitation; temperature).

Our study showed the ability of Sentinel-2 to support invasive alien plant mapping through a multitemporal approach supported by multispectral data together with vegeta-

tion and biophysical indices stacks, capable of feeding the *biomod2* fusion classifier. Overall, results show that the spatial, spectral, and temporal resolutions of Sentinel-2 were adequate for mapping *A. longfiolia* invaded areas, and it may be the case for similar plant species sharing similar compositional and structural traits [52].

However, contrary to what one would expect, the primary source of spectral information was not in the red, red-edge, or near-infrared regions (often valuable for depicting spectral information about concentrations of chlorophyll-a and other pigments typically used for vegetation analyses [52]). The Sentinel-2′s blue (458–523 nm), green (543–578 nm), and SWIR2 (2100–2280 nm) spectral bands were those that showed, for our study region and the period analyzed, better ability to discriminate between *A. longifolia* and other woody species.

A possible explanation for this fact is that *A. longifolia* fluorescence, like other yellow flowers, is better distinguished at the spectrum comprehend between 480–550 nm [63]. The carotenoids (yellow pigments) are known to cause high reflectance on the spectral region covered by the green light (due to decreased chlorophyll absorption of red light during senescence) and strong absorption in the blue light [64,65].

The SWIR2 spectral region is especially sensitive to vegetation water content and leaf liquid water and is often used for plant detection [66]. In our study, SWIR2 (band 12) obtained the best results in December and February, corresponding climatically to the rainy season and phenologically to the end of the growing period and the beginning of blooming.

Despite having contributed to improving image classification performance, the indices used were less relevant. This result may be because spectral information used for its calculation is also incorporated into the classification pipeline. Biophysical indices like LAI showed a good ability to distinguish areas invaded from the rest. A possible explanation is that LAI relates to the canopy structure, thus conveying useful vegetation structural features that allow disentangling the target species from other plant species. In addition, *A. longifolia* has been linked to broad biophysical changes in invaded areas, often with significant increases in leaf area index and reduced light intensity in the understory [35]. The same authors also describe profound changes in the water budget in invaded patches. Altogether, these effects may potentially explain the importance of LAI and the SWIR bands in image classification.

4.2. Landscape Patterns and Drivers of Acacia longifolia Distribution

The study area has a high level of occupation of *A. longifolia*, with stable populations capable of multiplying and spreading throughout the landscape. In particular, the spread of *A. longifolia*, according to our mapping results, poses a risk to various habitat types occurring in the territory, from coastal sand dunes, riparian corridors along streams and rivers, estuarine and wetland ecosystems (e.g., Natura 2000), and forest areas often along low-lying hillsides (e.g., Local Natural Monuments) [10].

In the study area, climatic drivers have the most decisive influence on explaining the target species distribution, with the coldest month's temperature being the most influential variable. Minimum temperatures can physiologically constrain plant function and are a well-known driver of landscape invasibility by frost-sensitive alien invaders [67,68]. However, in the face of global warming, with temperatures becoming warmer at higher altitudes, this abiotic barrier is in danger of decreasing and may increase the risk of invasion (i.e., upward elevation shift).

Drivers related to land cover/use also influence the abundance and spread of *A. longifolia* at the landscape level, as production forests such as eucalyptus (*Eucalyptus globulus)* or maritime pine (*Pinus pinaster*), widespread in the study area, are positively related to the species. Forest stands of (non-native) eucalyptus, often in monoculture, tend to present low species diversity [69] (due to inhibitory effects in plants [70]) and foster management practices with higher soil moving, which triggers conditions for the establishment of fast-growing species such as *A. longifolia* [71,72]. Eucalyptus plantations

often have a tree spacing and a canopy density that allows comparatively higher amounts of light to reach the understory stratum, thus facilitating *A. longifolia* development [73,74].

In contrast, shrubland areas were negatively related to the species coverage at the landscape level. This may happen due to the region's topography, where this land cover is linked to higher altitudes, translating into lower environmental suitability for the species because of lower minimum temperatures and higher difficulty for the seeds to reach these points. Nonetheless, these results deserve further study given *A. longifolia* ability to invade dune shrub ecosystems [33,35].

Landscape configuration and heterogeneity features are known to influence the spread and the extent of invaded areas [68,75]. We found that those landscapes with lower Shannon diversity, less patchy, and dominated by larger patches (i.e., higher mean patch area and a lower coefficient of variation) tend to be related to more invaded landscapes.

Lower levels of landscape heterogeneity promote the *A. longifolia* spread in the study area and may also increase the connectivity between and across *A. longifolia* populations, and was already identified as a driver positively influencing other Acacia species [71]. This effect may be linked to higher propagule availability from nearby populations, which increases the odds of establishment, persistence, naturalization, and invasion [76]. Besides, such results may be coherent with the non-long distance dispersal adaptation more often found in Acacia species, typically dispersed by animal vectors (e.g., birds and ants) [72].

Besides heterogeneity, other landscape features related to linear elements, such as rivers or motorways, were also positively linked to the species presence and spread. Despite obvious differences between dispersal agents and drivers acting in these two very distinct types of linear elements, both seem to promote pathways for the species spread at the landscape level [8,9], with implications for management and control actions [9].

As previously recorded for other Acacia species in Europe, fire disturbance was positively related to *A. longifolia* abundance [72]. In fact, this may connect to the species capacity to profit from disturbance (particularly in post-fire environments) with high-fire tolerance of the species, fast rate of vegetative reproduction, and allelopathic behavior [71,72].

4.3. Applications in Invasion Management and Control

Since *A. longifolia* is already widespread throughout the territory, in the short term, high-cost management is expected to implement control actions, particularly in production forest areas (economic impacts) and habitat types of high-conservation interest (ecological impacts). In the long term, costs will increase to further avoid the loss of relevant ecological values and their related services [77], reduce the effect of changes in fire frequency/risk [28,78], and decreasing soil formation in invaded areas [78]. If these losses are ignored or poorly tackled, tipping points may be unleashed, promoting regime shifts changing beyond return points ecosystem structure, function, or dynamics [79].

Managing alien plant invasions is a challenging process due to the multiscale processes acting across space and time. The early detection of invaded areas is the most cost-effective action but challenging to achieve due to a lack of monitoring programs dedicated to invasive alien species [68].

Monitoring actions in drivers related to land use and management (e.g., annual crops, production forest, discontinuous urban areas) may translate into time and efficiency gains. Overall, these spaces are of great importance for the containment of *A. longifolia*, due to their influence in invasibility patterns and for being drivers where political legislators and stakeholders can implement planning and action measures to control invasive alien plant species [80,81].

The mapping and quantification of invaded spaces may also allow the planning and adoption of large-scale actions to transform *A. longifolia*, using temporary economies, into an economic resource to self-finance recovery and restoration processes. The natural degradation process of *A. longifolia* in green waste compost leads to better soil quality and higher organic matter content, thus being a product of economic interest [82]. The high calorific potential of this species for the production of pellets is also known [83].

Nonetheless, using invasive alien species as an economic resource and market creation is always controversial and must be considered very carefully [84,85].

Besides abiotic and geographic variables that are impossible to control (e.g., climate, geomorphology, soil formation processes) and land use, other drivers related to landscape configuration like motorways and burnt areas play an essential role in the spread of *A. longifolia*. As such, these landscape elements and land use types should receive special attention from political decision-makers to effectively halt their spread.

4.4. Future Improvements to the Methodology

Improvements in the results obtained can be achieved by including free multi-sensor fusion (e.g., Sentinel-1 or Landsat) to have more features related to texture or a longer time span or resort to very-high spatial resolution images such as RapidEye or WorldView-2/3.

Future studies using the present methodology can explore the spatio-temporal transferability (for different regions and years) and the obtained distribution maps to identify more areas to collect ground-truth data aiming to complement the initial database and improve the image classification pipeline [86]. Assessing Sentinel-2 images' ability and limitations to map invaded areas with different plant sizes and densities is also a critical issue to target in future research. In addition, quantifying error propagation when using satellite-derived maps depicting invasion extent as inputs for modeling invasibility drivers is also highly relevant.

Predictive modeling can also be improved by incorporating variables with a higher spatial resolution (e.g., climate, land use/cover) and incorporating variables capable of describing human dynamics or pressures in the landscape (e.g., fire severity, land abandonment).

5. Conclusions

This study implemented a dual framework for improving the detection of invaded areas by *A. longifolia,* combining supervised image classification and a predictive modeling approach, respectively, to map the target species and to identify and rank the main drivers of abundance at the landscape level. By using Sentinel-2 multispectral data, we were able to discriminate invaded from non-invaded areas with very high sensitivity through *biomod2*'s package classifier fusion techniques and non-parametric ensemble classifiers. Overall, Sentinel-2's blue, green, and SWIR2 spectral bands for winter months (corresponding phenologically to the beginning of the growing period and blooming onset) presented the highest ability to discriminate between *A. longifolia* and the background vegetation.

Based on invaded areas maps and the Random Forest modeling algorithm, we were able to identify the most relevant drivers shaping the patterns of abundance of the target species in the study area. Models highlighted the primary role of climate (mainly of minimum temperatures), followed by landscape composition (fraction cover of production forest, shrublands, and artificialized areas) and landscape configuration (heterogeneity, patch size distribution, and density of linear elements) as the most important factors to explain the species' abundance at the landscape level.

The proposed dual framework combines image classification and predictive modeling into a single analytical pipeline, thus covering many of the requirements needed to support regional to global policy initiatives focused on prevention, early detection, and monitoring of invasions. Moreover, it strongly contributes to guiding local decision-making on early intervention for invasive species control by targeting and prioritizing the invaded areas while also tackling the primary environmental and anthropogenic drivers of the species' abundance and spread.

Table S3—Average driver importance ranking for all variables tested (ordered in descendent fashion), Table S4—Driver importance ranking for the 20-best selected variables for the final random forest model (ordered in descendent fashion), Figure S1—Partial dependence plots for all variables used in RF models, showing the relation between the response variable (abundance given by the percentage of invaded area, in the y-axis) and the selected predictive variables of different environmental factors (x-axis). The black line indicates the "raw" response from the RF model, while the blue line applies a moving average smooth.

Institutional Review Board Statement: Not applicable.

Informed Consent Statement: Not applicable.

Data Availability Statement: The data presented in this study are available on request from the corresponding author. The data are not publicly available due to legal (e.g., privacy) and ethical restrictions.

Conflicts of Interest: The authors declare no conflict of interest. The funders had no role in the design of the study; in the collection, analyses, or interpretation of data; in the writing of the manuscript, or in the decision to publish the results.

Appendix A

Table A1. Best variables in image ensemble classification selected from the preliminary analysis. The percentage shows the relative importance across all variables tested. The 17 variables with higher average importance combined perform approximately 45% of total importance.

Month/Spectral Band/Index	Average Variable Importance Score	Importance Score Standard Deviation	% Relative Importance
December_b12	0.137	0.206	4.79
January_b2	0.124	0.109	4.32
January_lai	0.120	0.183	4.18
April_b3	0.098	0.131	3.41
March_b3	0.084	0.162	2.94
December_b11	0.079	0.131	2.78
February_b9	0.070	0.133	2.44
December_b1	0.066	0.084	2.32
February_b12	0.065	0.132	2.29
March_b1	0.063	0.117	2.20
May_b3	0.061	0.127	2.14
December_b3	0.057	0.104	1.99
April_b2	0.054	0.065	1.89
February_b3	0.054	0.086	1.88
December_b4	0.048	0.075	1.69
March_lai	0.046	0.090	1.60
December_lai	0.045	0.097	1.60

Appendix B

Table A2. Full list of variables used for modelling landscape drivers of Acacia invasion, their acronyms and data sources.

Type	Acronym	Variable Description	Data Source
Climate	CL_BIO01	Annual Mean Temperature	CHELSA Climate data v-1.2 (URL: https://chelsa-climate.org/, access date: 6 December 2020, spatial resolution: ~1 Km^2, reference period: 1979–2013)
	CL_BIO02	Mean Diurnal Range (Mean of monthly (maximum temperature–minimum temperature))	
	CL_BIO03	Isothermality (CL_BIO2/CL_BIO7) (×100)	
	CL_BIO04	Temperature Seasonality (standard deviation × 100)	
	CL_BIO05	Maximum Temperature of Warmest Month	
	CL_BIO06	Minimum Temperature of Coldest Month	
	CL_BIO07	Temperature Annual Range (CL_BIO5–CL_BIO6)	
	CL_BIO08	Mean Temperature of Wettest Quarter	
	CL_BIO09	Mean Temperature of Driest Quarter	
	CL_BIO10	Mean Temperature of Warmest Quarter	
	CL_BIO11	Mean Temperature of Coldest Quarter	

Table A2. *Cont.*

Type	Acronym	Variable Description	Data Source
Climate	CL_BIO12	Annual Precipitation	
	CL_BIO13	Precipitation of Wettest Month	
	CL_BIO14	Precipitation of Driest Month	
	CL_BIO15	Precipitation Seasonality (Coefficient of Variation)	
	CL_BIO16	Precipitation of Wettest Quarter	
	CL_BIO17	Precipitation of Driest Quarter	
	CL_BIO18	Precipitation of Warmest Quarter	
	CL_BIO19	Precipitation of Coldest Quarter	
Disturbance	DT_BA10YR	Total Burnt Area (last 10 years)	Burnt Areas Dataset for Mainland Portugal (URL: https://geocatalogo.icnf.pt/, access date: 6 December 2020, spatial resolution: ~1 ha, reference period: 2000–2019)
	DT_BA20YR	Total Burnt Area (last 20 years)	
	DT_BA5YR	Total Burnt Area (last 5 years)	
Land use	LU_PCPCO	Percent cover of permanent crops	
	LU_PCACO	Percent cover of annual crops	
	LU_PCPAC	Percent cover of permanent and annual crops	
	LU_PCNFO	Percent cover of native forests	
	LU_PCEFO	Percent cover of eucalyptus (production) forest	
	LU_PCPFO	Percent cover of maritime-pine (production) forest	
	LU_PCSHL	Percent cover of shrublands	
	LU_PCAFM	Percent cover of complex agroforestry mosaics	
	LU_PCOPF	Percent cover of other production forests	Land Cover Map for Portugal (URL: http://mapas.dgterritorio.pt, access date: 11 December 2020: spatial resolution: ~100 m, reference year: 2018)
	LU_PCPAS	Percent cover of pasturelands	
	LU_PCWET	Percent cover of wetlands	
	LU_PCBSD	Percent cover of beaches and sand dunes	
	LU_PCRRL	Percent cover of roads and rails	
	LU_PCBRS	Percent cover of bare rock surfaces	
	LU_PCWTS	Percent cover of water surfaces	
	LU_PCART	Percent cover of artificial/urban areas	
	LU_PCSPV	Percent cover of sparsely vegetated areas	
Landscape pattern/ configuration and heterogeneity	LP_MNPAR	Landscape Mean Patch Area	
	LP_PACOV	Landscape Patch Area Coefficient of variation	
	LP_LAPAI	Landscape Largest Patch Index	
	LP_SHDVI	Landscape Shannon Diversity	
	LP_SPDVI	Landscape Simpson Diversity	
	LP_PASTD	Landscape Patch Area Standard-deviation	

Table A2. *Cont.*

Type	Acronym	Variable Description	Data Source
Linear elements	LE_EDGDN	Landscape edge density	
	LE_TLRIV	Total length of rivers	European River Catchment Database (URL: https://www.eea.europa.eu, access date: 6 December 2020: spatial resolution: 100 m, reference year: 2007)
	LE_TLROD	Total length of all road types	Open Street Map (URL: https://download.geofabrik.de/europe/portugal.html, access date: 6 December 2020: reference year: 2020)
	LE_TLMTW	Total length of motorways	
Soil properties	SO_AVWTC	Available water content	Topsoil physical properties for Europe (URL: https://esdac.jrc.ec.europa.eu, access date: 6 December 2020: spatial resolution: 500 m, reference year: 2009)
	SO_BULKD	Bulk Density	
	SO_PCLAY	Percent of clay in soils	
	SO_PCOAR	Percent of coarse elements in soils	
	SO_PSAND	Percent of sand in soils	
	SO_PSILT	Percent of silt in soils	
Topography/ Geomorphology	TG_SLOPE	Slope (%)	SRTM v-4.1 (URL: https://srtm.csi.cgiar.org/, access date: 6 December 2020: spatial resolution: 90 m, reference year: 2008)
	TG_RADAV	Average Solar Radiation	
	TG_TORGI	Topographic Ruggedness Index	
	TG_TOWTI	Topographic Wetness Index	

References

1. Vaz, A.S.; Kueffer, C.; Kull, C.A.; Richardson, D.M.; Vicente, J.R.; Kühn, I.; Schroter, M.; Hauck, J.; Bonn, A.; Honrado, J. Integrating ecosystem services and disservices: Insights from plant invasions. *Ecosyst. Serv.* **2017**, *23*, 94–107. [CrossRef]
2. Hulme, P.E.; Brundu, G.; Carboni, M.; Dehnen-Schmutz, K.; Dullinger, S.; Early, R.; Essl, F.; Gonzalez-Moreno, P.; Groom, Q.J.; Kueffer, C. Integrating invasive species policies across ornamental horticulture supply chains to prevent plant invasions. *J. Appl. Ecol.* **2018**, *55*, 92–98. [CrossRef]
3. Peerbhay, K.; Mutanga, O.; Lottering, R.; Bangamwabo, V.; Ismail, R. Detecting bugweed (Solanum mauritianum) abundance in plantation forestry using multisource remote sensing. *ISPRS J. Photogramm. Remote Sens.* **2016**, *121*, 167–176. [CrossRef]
4. McGeoch, M.A.; Genovesi, P.; Bellingham, P.J.; Costello, M.J.; McGrannachan, C.; Sheppard, A. Prioritizing species, pathways, and sites to achieve conservation targets for biological invasion. *Biol. Invasions* **2016**, *18*, 299–314. [CrossRef]
5. Brooks, M.L. Effects of Land Management Practices on Plant Invasions in Wildland Areas. In *Biological Invasions*; Springer: Berlin/Heidelberg, Germany, 2007; pp. 147–162.
6. Pyšek, P.; Richardson, D.M. Invasive Species, Environmental Change and Management, and Health. *Annu. Rev. Environ. Resour.* **2010**, *35*, 25–55. [CrossRef]
7. Milanović, M.; Knapp, S.; Pyšek, P.; Kühn, I. Linking traits of invasive plants with ecosystem services and disservices. *Ecosyst. Serv.* **2020**, *42*, 101072. [CrossRef]
8. Vicente, J.; Alves, P.; Randin, C.; Guisan, A.; Honrado, J. What drives invasibility? A multi-model inference test and spatial modelling of alien plant species richness patterns in northern Portugal. *Ecography* **2010**, *33*, 1081–1092. [CrossRef]
9. Vicente, J.R.; Pereira, H.M.; Randin, C.F.; Goncalves, J.; Lomba, A.; Alves, P.; Metzger, J.; Cezar, M.; Guisan, A.; Honrado, J. Environment and dispersal paths override life strategies and residence time in determining regional patterns of invasion by alien plants. *Perspect. Plant Ecol. Evol. Syst.* **2014**, *16*, 1–10. [CrossRef]
10. Souza-Alonso, P.; Rodríguez, J.; González, L.; Lorenzo, P. Here to stay. Recent advances and perspectives about Acacia invasion in Mediterranean areas. *Ann. For. Sci.* **2017**, *74*, 55. [CrossRef]
11. Marchante, E.; Marchante, H. Engaging Society to Fight Invasive Alien Plants in Portugal—One of the Main Threats to Biodiversity. In *World Sustainability Series*; Springer: Berlin/Heidelberg, Germany, 2016; pp. 107–122.
12. Nunes, L.R.; Meireles, C.I.R.; CJ, P.; NMC, A.R. Propagation Model of Invasive Species: Road Systems as Dispersion Facilitators. *Res. Ecol.* **2019**, *2*, 12–19. [CrossRef]
13. Alvarez-Taboada, F.; Paredes, C.; Julián-Pelaz, J. Mapping of the Invasive Species Hakea sericea Using Unmanned Aerial Vehicle (UAV) and WorldView-2 Imagery and an Object-Oriented Approach. *Remote Sens.* **2017**, *9*, 913. [CrossRef]
14. Royimani, L.; Mutanga, O.; Odindi, J.; Dube, T.; Matongera, T.N. Advancements in satellite remote sensing for mapping and monitoring of alien invasive plant species (AIPs). *Phys. Chem. Earth Parts A/B/C* **2019**, *112*, 237–245. [CrossRef]

15. Masemola, C.; Cho, M.A.; Ramoelo, A. Assessing the Effect of Seasonality on Leaf and Canopy Spectra for the Discrimination of an Alien Tree Species, Acacia Mearnsii, from Co-Occurring Native Species Using Parametric and Nonparametric Classifiers. *IEEE Trans. Geosci. Remote Sens.* **2019**, *57*, 5853–5867. [CrossRef]
16. Thuiller, W.; Lafourcade, B.; Engler, R.; Araújo, M.B. BIOMOD—A platform for ensemble forecasting of species distributions. *Ecography* **2009**, *32*, 369–373. [CrossRef]
17. Thuiller, W.; Georges, D.; Robin, E.; Breiner, F.; Engler, R.; Breiner, F. Package 'biomod2'. Ensemble Platform for Species Distribution Modeling. 2020. Available online: https://cran.r-project.org/web/packages/biomod2/biomod2.pdf (accessed on 10 August 2021).
18. Elith, J.; Leathwick, J.R. Species Distribution Models: Ecological Explanation and Prediction Across Space and Time. *Annu. Rev. Ecol. Evol. Syst.* **2009**, *40*, 677–697. [CrossRef]
19. Guisan, A.; Tingley, R.; Baumgartner, J.B.; Naujokaitis-Lewis, I.; Sutcliffe, P.R.; Tulloch, A.I.; Regan, T.J.; Brotons, L.; McDonald-Madden, E.; Mantyka-Pringle, C.; et al. Predicting species distributions for conservation decisions. *Ecol. Lett.* **2013**, *16*, 1424–1435. [CrossRef]
20. Barbosa, A.M.; Real, R.; Vargas, J.M. Use of Coarse-Resolution Models of Species' Distributions to Guide Local Conservation Inferences. *Conserv. Biol.* **2010**, *24*, 1378–1387. [CrossRef]
21. Hao, T.; Elith, J.; Guillera-Arroita, G.; Lahoz-Monfort, J.J. A review of evidence about use and performance of species distribution modelling ensembles like BIOMOD. *Divers. Distrib.* **2019**, *25*, 839–852. [CrossRef]
22. Löw, F.; Conrad, C.; Michel, U. Decision fusion and non-parametric classifiers for land use mapping using multi-temporal RapidEye data. *ISPRS J. Photogramm. Remote Sens.* **2015**, *108*, 191–204. [CrossRef]
23. Fernandes, R.F.; Vicente, J.R.; Georges, D.; Alves, P.; Thuiller, W.; Honrado, J.P. A novel downscaling approach to predict plant invasions and improve local conservation actions. *Biol. Invasions* **2014**, *16*, 2577–2590. [CrossRef]
24. Huang, C.; Asner, G. Applications of Remote Sensing to Alien Invasive Plant Studies. *Sensors* **2009**, *9*, 4869–4889. [CrossRef]
25. Vicente, J.; Randin, C.F.; Gonçalves, J.; Metzger, M.J.; Lomba, Â.; Honrado, J.; Guisan, A. Where will conflicts between alien and rare species occur after climate and land-use change? A test with a novel combined modelling approach. *Biol. Invasions* **2011**, *13*, 1209–1227. [CrossRef]
26. Shmueli, G. To Explain or to Predict? *Stat. Sci.* **2010**, *25*, 289–310. [CrossRef]
27. Monteiro, A.T.; Gonçalves, J.; Fernandes, R.F.; Alves, S.; Marcos, B.; Lucas, R.; Teodoro, A.C.; Honrado, J. Estimating Invasion Success by Non-Native Trees in a National Park Combining WorldView-2 Very High Resolution Satellite Data and Species Distribution Models. *Diversity* **2017**, *9*, 6. [CrossRef]
28. Le Maitre, D.C.; Gaertner, M.; Marchante, E.; Ens, E.J.; Holmes, P.M.; Pauchard, A.; O'Farrell, P.J.; Rogers, A.M.; Blanchard, R.; Blignaut, J.; et al. Impacts of invasive Australian acacias: Implications for management and restoration. *Divers. Distrib.* **2011**, *17*, 1015–1029. [CrossRef]
29. Shamsbiranvand, M.-H.; Khodadadi, A.; Assarehzadegan, M.-A.; Borsi, S.H.; Amini, A. Immunochemical Characterization of Acacia Pollen Allergens and Evaluation of Cross-Reactivity Pattern with the Common Allergenic Pollens. *J. Allergy* **2014**, *2014*, 409056. [CrossRef]
30. Irian, S.; Majd, A.; Hoseinizadeh, A.; Jonubi, P. A study on the allergenicity and ontogeny of Acacia farnesiana pollen grains in guinea pigs. *Aerobiologia* **2013**, *29*, 21–29. [CrossRef]
31. Mkunyana, Y.P.; Mazvimavi, D.; Dzikiti, S.; Ntshidi, Z. A comparative assessment of water use by Acacia longifolia invasions occurring on hillslopes and riparian zones in the Cape Agulhas region of South Africa. *Phys. Chem. Earth Parts A/B/C* **2019**, *112*, 255–264. [CrossRef]
32. Lazzaro, L.; Giuliani, C.; Fabiani, A.; Agnelli, A.E.; Pastorelli, R.; Lagomarsino, A.; Benesperi, R.; Calamassi, R.; Foggi, B. Soil and plant changing after invasion: The case of Acacia dealbata in a Mediterranean ecosystem. *Sci. Total Environ.* **2014**, *497*, 491–498. [CrossRef]
33. Marchante, E.; Kjøller, A.; Struwe, S.; Freitas, H. Short- and long-term impacts of Acacia longifolia invasion on the belowground processes of a Mediterranean coastal dune ecosystem. *Appl. Soil Ecol.* **2008**, *40*, 210–217. [CrossRef]
34. Rascher, K.G.; Große-Stoltenberg, A.; Máguas, C.; Werner, C. Understory Invasion by Acacia longifolia Alters the Water Balance and Carbon Gain of a Mediterranean Pine Forest. *Ecosystems* **2011**, *14*, 904–919. [CrossRef]
35. Rascher, K.G.; Große-Stoltenberg, A.; Máguas, C.; Meira-Neto, J.A.A.; Werner, C. Acacia longifolia invasion impacts vegetation structure and regeneration dynamics in open dunes and pine forests. *Biol. Invasions* **2011**, *13*, 1099–1113. [CrossRef]
36. Fernandes, M.M. Acácias e geografia histórica: Rotas de um percurso. *Cad. Curso Doutor. Geogr.* **2012**, *4*, 23–40.
37. Vicente, J.R.; Fernandes, R.F.; Randin, C.F.; Broennimann, O.; Gonçalves, J.; Marcos, B.; Pocas, I.; Alves, P.; Guisan, A.; Honrado, J.P. Will climate change drive alien invasive plants into areas of high protection value? An improved model-based regional assessment to prioritise the management of invasions. *J. Environ. Manag.* **2013**, *131*, 185–195. [CrossRef] [PubMed]
38. Santos, M.; Freitas, R.; Crespí, A.L.; Hughes, S.J.; Cabral, J.A. Predicting trends of invasive plants richness using local socio-economic data: An application in North Portugal. *Environ. Res.* **2011**, *111*, 960–966. [CrossRef]
39. De Sá, N.C.; Marchante, H.; Marchante, E.; Cabral, J.A.; Honrado, J.P.; Vicente, J.R. Can citizen science data guide the surveillance of invasive plants? A model-based test with Acacia trees in Portugal. *Biol. Invasions* **2019**, *21*, 2127–2141. [CrossRef]
40. Estado do Ordenamento do Território—Câmara Municipal de Viana do Castelo. 2019. Available online: http://www.cm-viana-castelo.pt/pt/estado-do-ordenamento-do-territorio (accessed on 29 June 2020).

41. Große-Stoltenberg, A.; Hellmann, C.; Thiele, J.; Werner, C.; Oldeland, J. Early detection of GPP-related regime shifts after plant invasion by integrating imaging spectroscopy with airborne LiDAR. *Remote Sens. Environ.* **2018**, *209*, 780–792. [CrossRef]
42. Barbet-Massin, M.; Jiguet, F.; Albert, C.H.; Thuiller, W. Selecting pseudo-absences for species distribution models: How, where and how many? *Methods Ecol. Evol.* **2012**, *3*, 327–338. [CrossRef]
43. Main-Knorn, M.; Pflug, B.; Louis, J.; Debaecker, V.; Müller-Wilm, U.; Gascon, F. Sen2Cor for Sentinel-2. In *Image and Signal Processing for Remote Sensing XXIII*; SPIE Remote Sensing: Warsaw, Poland, 2017; p. 10427.
44. Lanaras, C.; Bioucas-Dias, J.; Galliani, S.; Baltsavias, E.; Schindler, K. Super-resolution of Sentinel-2 images: Learning a globally applicable deep neural network. *ISPRS J. Photogramm. Remote Sens.* **2018**, *146*, 305–319. [CrossRef]
45. Henrich, V.; Jung, A.; Götze, C.; Sandow, C.; Thürkow, D.; Gläßer, C. Development of an Online Indices Database: Motivation, Concept and Implementation. In Proceedings of the 6th EARSeL Imaging Spectroscopy SIG Workshop Innovative Tool for Scientific and Commercial Environment Applications, Tel Aviv, Israe, 16–19 March 2009; pp. 16–18.
46. Wilfong, B.N.; Gorchov, D.L.; Henry, M.C. Detecting an Invasive Shrub in Deciduous Forest Understories using Remote Sensing. *Weed Sci.* **2009**, *57*, 512–520. [CrossRef]
47. Savage, S.L.; Lawrence, R.L. Vegetation Dynamics in Yellowstone's Northern Range: 1985 to 1999. *Photogramm. Eng. Remote Sens.* **2010**, *76*, 547–556. [CrossRef]
48. Underwood, E. Mapping nonnative plants using hyperspectral imagery. *Remote Sens. Environ.* **2003**, *86*, 150–161. [CrossRef]
49. Ai, J.; Gao, W.; Shi, R.; Zhang, C.; Sun, Z.; Chen, W.; Liu, C.; Zeng, Y. In Situ Hyperspectral Data Analysis for Canopy Chlorophyll Content Estimation of an Invasive Species Spartina Alterniflora based on PROSAIL Canopy Radiative Transfer Model. In *Remote Sensing and Modeling of Ecosystems for Sustainability XII*; SPIE Optical Engineering: San Diego, CA, USA, 2015; Volume 9610, p. 961007.
50. Main, R.; Cho, M.A.; Mathieu, R.; O'Kennedy, M.M.; Ramoelo, A.; Koch, S. An investigation into robust spectral indices for leaf chlorophyll estimation. *ISPRS J. Photogramm. Remote Sens.* **2011**, *66*, 751–761. [CrossRef]
51. Qi, J.; Chehbouni, A.; Huete, A.R.; Kerr, Y.H.; Sorooshian, S. A modified soil adjusted vegetation index. *Remote Sens. Environ.* **1994**, *48*, 119–126. [CrossRef]
52. Masemola, C.; Cho, M.A.; Ramoelo, A. Towards a semi-automated mapping of Australia native invasive alien Acacia trees using Sentinel-2 and radiative transfer models in South Africa. *ISPRS J. Photogramm. Remote Sens.* **2020**, *166*, 153–168. [CrossRef]
53. Gómez, C.; White, J.C.; Wulder, M.A. Optical remotely sensed time series data for land cover classification: A review. *ISPRS J. Photogramm. Remote Sens.* **2016**, *116*, 55–72. [CrossRef]
54. Liu, C.; Berry, P.M.; Dawson, T.P.; Pearson, R.G. Selecting thresholds of occurrence in the prediction of species distributions. *Ecography* **2005**, *28*, 385–393. [CrossRef]
55. Gormley, A.M.; Forsyth, D.M.; Griffioen, P.; Lindeman, M.; Ramsey, D.S.; Scroggie, M.P.; Woodford, L. Using presence-only and presence-absence data to estimate the current and potential distributions of established invasive species. *J. Appl. Ecol.* **2011**, *48*, 25–34. [CrossRef]
56. Allouche, O.; Tsoar, A.; Kadmon, R. Assessing the accuracy of species distribution models: Prevalence, kappa and the true skill statistic (TSS). *J. Appl. Ecol.* **2006**, *43*, 1223–1232. [CrossRef]
57. Breiman, L. Random forests. *Mach. Learn.* **2001**, *45*, 5–32. [CrossRef]
58. Kuhn, M.; Johnson, K. *Applied Predictive Modeling*; Springer: New York, NY, USA, 2013.
59. Greenwell, B.M. pdp: An R package for constructing partial dependence plots. *R J.* **2017**, *9*, 421–436. [CrossRef]
60. Bolch, E.A.; Santos, M.J.; Ade, C.; Khanna, S.; Basinger, N.T.; Reader, M.O.; Hestir, E.L. Remote Detection of Invasive Alien Species. In *Remote Sensing of Plant Biodiversity*; Springer International Publishing: Cham, Switzerland, 2020; pp. 267–307.
61. Rocchini, D.; Andreo, V.; Förster, M.; Garzon-Lopez, C.X.; Gutierrez, A.P.; Gillespie, T.W.; Hauffe, H.C.; He, K.S.; Kleinschmit, B.; Mairota, P.; et al. Potential of remote sensing to predict species invasions: A modelling perspective. *Prog. Phys. Geogr.* **2015**, *39*, 283–309. [CrossRef]
62. Rocchini, D.; Petras, V.; Petrasova, A.; Horning, N.; Furtkevicova, L.; Neteler, M.; Leutner, B.; Wegmann, M. Open data and open source for remote sensing training in ecology. *Ecol. Inform.* **2017**, *40*, 57–61. [CrossRef]
63. Sulik, J.J.; Long, D.S. Spectral indices for yellow canola flowers. *Int. J. Remote Sens.* **2015**, *36*, 2751–2765. [CrossRef]
64. Mahmud, M.R.; Numata, S.; Hosaka, T. Mapping an invasive goldenrod of Solidago altissima in urban landscape of Japan using multi-scale remote sensing and knowledge-based classification. *Ecol. Indic.* **2020**, *111*, 105975. [CrossRef]
65. Misra, G.; Cawkwell, F.; Wingler, A. Status of Phenological Research Using Sentinel-2 Data: A Review. *Remote Sens.* **2020**, *12*, 2760. [CrossRef]
66. Wang, B.; Jia, K.; Liang, S.; Xie, X.; Wei, X.; Zhao, X.; Yao, Y.; Zhang, X. Assessment of Sentinel-2 MSI Spectral Band Reflectances for Estimating Fractional Vegetation Cover. *Remote Sens.* **2018**, *10*, 1927. [CrossRef]
67. Pino, J.; Font, X.; Carbó, J.; Jové, M.; Pallarès, L. Large-scale correlates of alien plant invasion in Catalonia (NE of Spain). *Biol. Conserv.* **2005**, *122*, 339–350. [CrossRef]
68. Vicente, J.R.; Kueffer, C.; Richardson, D.M.; Vaz, A.S.; Cabral, J.A.; Hui, C.; Araujo, M.B.; Kuhn, I.; Kull, C.A.; Verburg, P.H.; et al. Different environmental drivers of alien tree invasion affect different life-stages and operate at different spatial scales. *For. Ecol. Manag.* **2019**, *433*, 263–275. [CrossRef]
69. Proença, V.M.; Pereira, H.M.; Guilherme, J.; Vicente, L. Plant and bird diversity in natural forests and in native and exotic plantations in NW Portugal. *Acta Oecol.* **2010**, *36*, 219–226. [CrossRef]

70. Becerra, P.I.; Catford, J.A.; Luce McLeod, M.; Andonian, K.; Aschehoug, E.T.; Montesinos, D.; Callaway, R.M. Inhibitory effects of Eucalyptus globulus on understorey plant growth and species richness are greater in non-native regions. *Glob. Ecol. Biogeogr.* **2018**, *27*, 68–76. [CrossRef]

71. Hernández, L.; Fernández, J.M.; Cañellas, I.; de la Cueva, A.V. Assessing spatio-temporal rates, patterns and determinants of biological invasions in forest ecosystems. The case of Acacia species in NW Spain. *For. Ecol. Manag.* **2014**, *329*, 206–213. [CrossRef]

72. Lorenzo, P.; González, L.; Reigosa, M.J. The genus Acacia as invader: The characteristic case of Acacia dealbata Link in Europe. *Ann. For. Sci.* **2010**, *67*, 101. [CrossRef]

73. Sebert-Cuvillier, E.; Simon-Goyheneche, V.; Paccaut, F.; Chabrerie, O.; Goubet, O.; Decocq, G. Spatial spread of an alien tree species in a heterogeneous forest landscape: A spatially realistic simulation model. *Landsc. Ecol.* **2008**, *23*, 787–801. [CrossRef]

74. With, K.A. The Landscape Ecology of Invasive Spread. *Conserv. Biol.* **2002**, *16*, 1192–1203. [CrossRef]

75. Guillerme, S.; Barcet, H.; de Munnik, N.; Maire, E.; Marais-Sicre, C. Evolution of traditional agroforestry landscapes and development of invasive species: Lessons from the Pyrenees (France). *Sustain. Sci.* **2020**, *15*, 1285–1299. [CrossRef]

76. Alston, K.P.; Richardson, D.M. The roles of habitat features, disturbance, and distance from putative source populations in structuring alien plant invasions at the urban/wildland interface on the Cape Peninsula, South Africa. *Biol. Conserv.* **2006**, *132*, 183–198. [CrossRef]

77. Marchante, H.; Marchante, E.; Freitas, H.; Hoffmann, J.H. Temporal changes in the impacts on plant communities of an invasive alien tree, Acacia longifolia. *Plant Ecol.* **2015**, *216*, 1481–1498. [CrossRef]

78. Castro-Díez, P.; Alonso, Á.; Saldaña-López, A.; Granda, E. Effects of widespread non-native trees on regulating ecosystem services. *Sci. Total Environ.* **2021**, *778*, 146141. [CrossRef]

79. Moore, J.C. Predicting tipping points in complex environmental systems. *Proc. Natl. Acad. Sci. USA* **2018**, *115*, 635–636. [CrossRef] [PubMed]

80. Heringer, G.; Thiele, J.; do Amaral, C.H.; Meira-Neto, J.A.A.; Matos, F.A.R.; Lehmann, J.R.K.; Buttschardt, T.K.; Neri, A.V. Acacia invasion is facilitated by landscape permeability: The role of habitat degradation and road networks. *Appl. Veg. Sci.* **2020**, *23*, 598–609. [CrossRef]

81. Sánchez-Ortiz, K.; Taylor, K.J.; De Palma, A.; Essl, F.; Dawson, W.; Kreft, H.; Pergl, J.; Pysek, P.; Kleunen, M.V.; Weigelt, P.; et al. Effects of land-use change and related pressures on alien and native subsets of island communities. *PLoS ONE* **2020**, *15*, e0227169. [CrossRef] [PubMed]

82. Brito, L.M.; Reis, M.; Mourão, I.; Coutinho, J. Use of Acacia Waste Compost as an Alternative Component for Horticultural Substrates. *Commun. Soil Sci. Plant Anal.* **2015**, *46*, 1814–1826. [CrossRef]

83. Nunes, L.J.R.; Raposo, M.A.M.; Meireles, C.I.R.; Gomes, C.J.P.; Ribeiro, N.M.C.A. Control of Invasive Forest Species through the Creation of a Value Chain: Acacia dealbata Biomass Recovery. *Environments* **2020**, *7*, 39. [CrossRef]

84. Barnes, M.A.; Deines, A.M.; Gentile, R.M.; Grieneisen, L.E. Adapting to Invasions in a Changing World: Invasive Species as an Economic Resource. In *Invasive Species and Global Climate Change*; CAB International: Wallingford, UK, 2014; pp. 326–344.

85. Nuñez, M.A.; Kuebbing, S.; Dimarco, R.D.; Simberloff, D. Invasive Species: To eat or not to eat, that is the question. *Conserv. Lett.* **2012**, *5*, 334–341. [CrossRef]

86. Guisan, A.; Broennimann, O.; Engler, R.; Vust, M.; Yoccoz, N.G.; Lehmann, A.; Zimmermann, N.E. Using Niche-Based Models to Improve the Sampling of Rare Species. *Conserv. Biol.* **2006**, *20*, 501–511. [CrossRef]